

**Characterization of three druggable hotspots in the Aurora-A/TPX2 interaction
using biochemical, biophysical and fragment-based approaches**

**Patrick J. McIntyre¹, Patrick M. Collins², Lukáš Vrzal^{3,4}, Kristian Birchall⁵,
Laurence H. Arnold⁵, Chido Mpamhanga⁵, Peter J. Coombs⁵, Selena G.
Burgess⁶, Mark W. Richards⁶, Anja Winter¹, Václav Veverka⁴, Frank von
Delft^{2,7,8}, Andy Merritt⁵ and Richard Bayliss⁶**

¹Department of Molecular and Cell Biology, Henry Wellcome Building, University of
Leicester, Leicester, LE1 9HN, United Kingdom

²Diamond Light Source, Harwell Science and Innovation Campus, Didcot, OX11
0DE, United Kingdom

³University of Chemistry and Technology, Technická 5, Prague 6 - Dejvice, Prague,
166 28, Czech Republic

⁴Institute of Organic Chemistry and Biochemistry, Flemingovo nám. 542/2, Prague 6,
Prague, 166 10, Czech Republic

⁵LifeArc (Formerly MRC Technology), Stevenage Bioscience Catalyst, Gunnels
Wood Road, Stevenage, SG1 2FX, United Kingdom

⁶Astbury Centre for Structural and Molecular Biology, School of Molecular and
Cellular Biology, Faculty of Biological Sciences, University of Leeds, Leeds LS2 9JT,
United Kingdom

⁷Structural Genomics Consortium, Nuffield Department of Medicine,
University of Oxford, Roosevelt Drive, Oxford, OX3 7DQ, UK

⁸Department of Biochemistry, University of Johannesburg, Auckland Park, 2006,
South Africa

To whom correspondence should be addressed: Prof. Richard Bayliss, Astbury Centre for
Structural and Molecular Biology, School of Molecular and Cellular Biology, Faculty of
Biological Sciences, University of Leeds, Leeds LS2 9JT, United Kingdom. E-mail:
r.w.bayliss@leeds.ac.uk

SUPPLEMENTARY RESULTS AND DISCUSSION

Quantification of the contributions in binding made by residues in the Aurora-A/TPX2 interface – A crystal structure of the complex between phosphorylated Aurora-A and TPX2 shows molecular interactions involving three pockets on the Aurora-A surface named here as the Y-, F- and W-pockets for the key amino acids in TPX2 that interact with each pocket (Figure 1A). However, the contribution of each of these binding sites to the affinity of the interaction is unknown. We therefore introduced a series of mutations into a fragment encompassing the first 43 residues of TPX2 and analysed the interactions of these mutants with Aurora-A^{CA} (a C290A, C393A double point mutant of the Aurora-A kinase domain) by co-precipitation assay (Figure 1B, Table 1). All of the mutants tested exhibited reduced binding relative to wild-type TPX2, although the effect varied greatly. Mutation of Asp11 had the smallest effect on binding. Complete loss of functionality through mutation to alanine (mutant D11A) reduced binding to Aurora-A^{CA} by 1/2 and altering the functionality at this position, either by adjusting the length or the charge of the side-chain (mutants D11E and D11N, respectively) both reduced binding by 1/3. Loss of functionality of the other residues had a larger negative impact on Aurora-A^{CA} binding. Mutation of Phe16, Trp34 or Phe35 to alanine resulted in a reduction in Aurora-A^{CA} binding by 60-70%, indicating that these three sites are more important than Asp11 for complex formation. Aurora-A^{CA} binding was reduced by >80% when Tyr10 or Phe19 was mutated to alanine, indicating that these residues are critical in the Aurora-A/TPX2 interaction.

Further analysis of the ITC binding data

Examination of the enthalpic and entropic terms of binding between the TPX2 mutants and Aurora-A also reveals interesting details about the interaction, although the interpretation is complicated by, in some cases, large differences in these terms from the wild-type TPX2 (Table 1). Mutations of the residues that bind the Y-pocket of Aurora-A, Tyr8 and Tyr10, exhibit less favourable enthalpic terms, consistent with the extensive buried surface area of this region of the interaction. However, this is offset by an increase in the entropic contribution to the interaction. Unexpectedly, mutations of the residues that interact with the F-pocket (Phe16, Phe19) exhibit more favourable enthalpic contributions to binding, but much less favourable entropic terms. This is likely to be because, unlike the residues that interact with the Y-pocket, the side chains of Phe16 and Phe19 also form intramolecular interactions which may

pre-order of this region of TPX2 in a manner that is disrupted by mutation of these residues to alanine. Mutations in the residues that interact with the W-pocket, Trp34 and Phe35, produce surprisingly different changes in the entropic and enthalpic components suggesting that, while the tryptophan side chain contributes to both components of ΔG , the phenylalanine side chain contributes most through entropy of binding. We are cautious about these interpretations, and more robust insights into the thermodynamic contributions of individual TPX2 side chains would require further studies.

SUPPLEMENTARY METHODS

Purification of Aurora-A. Unless stated otherwise, all Aurora-A expressed, purified and used for any assays in this work is a variant consisting of residues 122-403 containing mutations C290A and C393A and phosphorylated on Thr288 during expression in *E. coli* (Aurora-A^{CA}) (S1). This mutant has enhanced stability, compared to wild-type Aurora-A, that makes it more suitable for *in vitro* biophysical studies (S2). N-terminally His₆-tagged Aurora-A was expressed from a version of pET30 (Novagen) in *Escherichia coli* and purified as described in (S3). Briefly, a cell pellet from 2 litres of culture was resuspended in 25 mL buffer A (50 mM Tris, pH 7.5; 40 mM imidazole; 300 mM NaCl; 5 mM MgCl₂; 10% w/v glycerol) with one tablet of Complete™ EDTA free Protease Inhibitor Cocktail (Roche) added. The clarified lysate was filtered (0.45 μ m membrane) and then loaded onto a HisTrap HP 5 mL column (GE Healthcare) before being washed with buffer A and then eluted using an increasing gradient of buffer B (buffer A supplemented with 500 mM imidazole). Pooled fractions containing protein were concentrated to 5 mL using a 10 kDa MW cut-off Vivaspin spin column and injected into and eluted through a 26/60 Sephacryl S200 column (GE Healthcare) with gel filtration buffer (20 mM Tris, pH 7.0; 200 mM NaCl; 5 mM MgCl₂; 5 mM 2-mercaptoethanol; 10% w/v glycerol). High purity Aurora-A containing fractions were pooled, concentrated and flash-frozen for future use.

Purification of TPX2¹⁻⁴³. The TPX2 construct used comprised residues 1-43 with an N-terminal glutathione S-transferase (GST) fusion (S4) in a

pGEX plasmid (GE Healthcare). GST-tagged TPX2 protein was expressed in *Escherichia coli* and the cleared lysate added to Glutathione Sepharose resin (GE Healthcare) pre-equilibrated in buffer C (50 mM Tris, pH 7.5; 300 mM NaCl). The suspension was agitated for three hours at 4 °C before the flow-through was removed and the remaining beads were washed with 10 column volumes of buffer C. To obtain GST-tagged TPX2, the resin was incubated in 5 column volumes of elution buffer (50 mM Tris, pH 8.0; 10 mM reduced glutathione) for 1 hour and the flowthrough was concentrated to ~5 mL before being passed through a 26/60 Sephacryl S200 column (GE Healthcare) equilibrated in buffer C. To obtain untagged TPX2, His₆-tagged TEV protease (0.5 mL, 1 mg/mL) was added to the GST-TPX2-bound resin in 3.5 mL of buffer C and the suspension incubated with agitation overnight at 4 °C. The flow-through was collected and the beads washed with 5 column volumes of buffer C. All fractions were passed through a HisTrap HP 5 mL column to remove the TEV protease. TPX2 proteins were concentrated, aliquoted and flash-frozen in liquid nitrogen for storage at -80 °C.

Mutagenesis. Mutations to Aurora-A and TPX2 were made using the QuikChange method (Stratagene).

Co-precipitation assays. Co-precipitation assays were performed by binding 30 µg GST or GST-TPX2 to 25 µL Glutathione Sepharose beads equilibrated in 250 µL binding buffer (PBS; 0.05% Tween 20; 2 mM DTT) at 4 °C for 1 hour. The beads were washed three times with binding buffer and then 25 µg Aurora-A^{CA} and 250 µL binding buffer were added to the beads. After incubation at 4 °C for 1 hour, the beads were washed three times with binding buffer before analysis by SDS-PAGE. Protein bands were quantified using ImageJ software and standardised against wild-type Aurora-A^{CA}/TPX2 complex.

Isothermal titration calorimetry (ITC). ITC experiments were carried out using a MicroCal VP-ITC system (GE Healthcare) at 20 °C. Both Aurora-A and cleaved TPX2 were dialysed into ITC buffer overnight (20 mM Sodium phosphate, pH 7; 200 mM NaCl; 5 mM MgCl₂; 10 % v/v glycerol). Initially the

cell was filled with 10 μM of either Aurora-A or TPX2 and the syringe was loaded with the second protein at 100 μM . If satisfactory binding saturation was not obtained then the concentrations of cell and syringe protein were altered. In the fragment-containing titrations, compounds were included as close to 25 mM as their solubility would allow, mostly at 5 % DMSO but for some particularly insoluble compounds the final DMSO concentration was 10 %. In each experiment, the equivalent amount of DMSO was added to the cell sample to prevent DMSO-related buffer mismatch between the cell and syringe samples. An initial injection of 3 μL was followed by 13 injections of 7 μL and then 16 injections of 14 μL . All injections lasted 2 seconds per μL with 240 seconds delay between each injection. Syringe rotation speed was 300 rpm throughout. The signal for the enthalpy of dilution of protein into buffer was measured and deemed negligible compared to the signal for the enthalpy of binding of the two proteins. For the fragment-containing experiments this was not the case and the signals obtained from a fragment-into-buffer control titration were subtracted from the experimental fragment traces. The K_d was determined using a nonlinear regression fit of the data using a single-site binding model within Origin software (Microcal). For all fragment experiments, the stoichiometry was fixed at 1:1 for curve fitting with the exception of Fragment 1 which was not restrained and showed a stoichiometry of 0.43:1. The wild-type experiment was performed at least in triplicate, the Aurora-A mutant and dephosphorylation experiments at least in duplicate and each TPX2 mutant experiment was performed only once. The fragment-binding experiments were performed between 1-3 times depending on the fragment. The K_d values shown are either the mean of multiple K_d measurements \pm standard deviation or, where only one experiment was performed, the K_d value calculated from that experiment \pm the error of curve fitting.

NMR-STD. For the validation experiments, samples contained Aurora-A^{CA} (5 μM), fragment (500 μM), 5% v/v D₂O and 5% v/v D₆-DMSO in NMR buffer (20 mM potassium phosphate, pH 7.0, 50 mM NaCl). Control samples containing no protein were made for each fragment. ¹H and STD spectra were recorded at 299.3 K on a 600 MHz Bruker spectrometer fitted with a cryo-probe and analysed by TopSpin (v3.2) software.

The duration of the ^1H 90° pulse was 10.70 μs . The ^1H STD spectrum was obtained using a standard pulse sequence with on-resonance irradiation at 0 ppm and off-resonance irradiation at 45 ppm. A train of 90° Gaussian pulses of 50 ms applied for 6 s was used for selective saturation. A relaxation delay of 10 s and 96 transients were used for the difference spectrum. Spinlock was used to suppress protein signals. The difference spectrum was obtained by direct subtraction of the on-resonance spectrum from the off-resonance spectrum. An STD response was noted if peaks corresponding to any seen in the ^1H spectrum of a fragment could be seen in the difference spectrum. A signal/noise ratio of at least 2 was applied as the lowest limit for definition of a peak. To quantify the STD response of a fragment, the integrals of the peaks in the difference spectrum and the off-resonance spectrum were calculated and the area of the difference spectrum peak expressed as a percentage of its corresponding off-resonance peak.

Activity assay (ADP-QuestTM). IC_{50} values for each fragment against Aurora-A^{CA} and the Aurora-A^{CA}/TPX2 complex were calculated using the ADP QuestTM kit (DiscoverX) in kinetic mode. A 10 μL reaction volume was made containing protein (Aurora-A at 500 nM, TPX2 at 600 nM), fragment (ranging from 2 mM to 64 nM, final DMSO at 5%) and ATP (50 μM) in gel filtration buffer (as described above but without the 2-mercaptoethanol). Protein and fragment were incubated together at room temperature for 30 minutes before the addition of 5 μL of 'Reagent A', 10 μL of 'Reagent B' and finally the ATP. Kinase activity was measured as fluorescence, proportional to the amount of ADP being generated. 'Fluorescence' versus 'Time' was plotted to calculate the linear rate of each well and this was then converted to '% of control activity' using the 'no fragment' and 'no protein' control wells and plotted versus concentration to give the IC_{50} of each fragment in duplicate.

Crystallisation. Crystals of Aurora-A^{CA} in complex with ADP were grown at 22 $^\circ\text{C}$ by sitting drop vapour diffusion in a 0.25 μL + 0.25 μL mixture of mother liquor (0.1 M Tris, pH 8.5; 0.5 M NaCl; 0.2 M MgCl_2 ; 32.5% v/v PEG 3350) and protein solution (600 μM Aurora-A^{CA}; 5 mM ADP; 5 mM MgCl_2) in SwissCi/MRC 3-well plates to give as high a yield of crystal-containing drops

per plate as possible.

XChem fragment screening. All methodology details of the XChem fragment screening platform can be found on its dedicated webpage, accessible from the Diamond Light Source homepage. Briefly, all drops were first photographed by imaging software before being ranked according to the presence and quality of crystals by TeXRank (S5). An ECHO acoustic liquid handler (Labcyte) was used to transfer individual fragments to crystal drops, aiming for an area of the drop that would cause minimum disruption to the crystal, as determined by visual inspection following the TeXRank step (S6). Crystals were soaked for 3 hours with two fragment libraries; the Diamond-SGC Poised Library set of 255 fragments (at the time of the experiment) and the Maybridge 1000 set of 1000 fragments with final fragment concentrations of 200 and 80 mM, respectively, with DMSO at 40% v/v. After soaking, crystals were mounted and cryo-cooled (with no additional cryoprotectant added) into pucks, with all data then collected on beamline I04-1 in 'automated unattended' mode. Autoprocessed datasets were processed by PanDDA (S7) in XChemExplorer (S8) which revealed clear electron density for any bound fragments. Structure solution by molecular replacement was performed with PDB: 4CEG as the search model. Structural modelling and refinement were performed using Phenix (S9) and Coot (S10).

Supplementary Table S1. Thermodynamic parameters for binding of wild-type TPX2 to phosphorylated and dephosphorylated Aurora-A variants C290A/C393A, R180A and R286A as determined by ITC.

Aurora-A variant	K_a ($10^3 M^{-1}$)	ΔH (kcal mol ⁻¹)	$-\Delta S$ (kcal mol ⁻¹)	K_d (μM)	N
Phosphorylated	4182.50 ± 635.00	-22.29 ± 0.34	13.40	0.27 ± 0.04	0.95
Dephosphorylated	428.00 ± 45.33	-31.97 ± 1.15	24.40	2.46 ± 0.26	0.76
R180A	168.67 ± 13.67	-38.49 ± 1.91	31.50	6.16 ± 0.52	0.61
R180A (Dephos)	189.67 ± 46.27	-27.71 ± 3.33	20.67	6.99 ± 1.20	1.00
R286A	286.67 ± 28.00	-40.18 ± 1.27	32.82	3.55 ± 0.33	0.77
R286A (Dephos)	408.00 ± 31.00	-30.73 ± 0.47	23.31	2.66 ± 0.21	0.86

K_a , binding constant; ΔH and ΔS , enthalpic and entropic terms; $T = 293 K$; N , the stoichiometry derived from the curve fitting of each interaction; K_d , dissociation constant. 'Phosphorylated' and 'Dephosphorylated' variants refer to Aurora-A^{CA} whereas both R180A and R286A mutations were made in a wild-type kinase domain construct. (Dephos) is shorthand for dephosphorylated, if not specified then phosphorylated is assumed. All experiments were performed at least in duplicate. The errors given by Origin curve-fitting software for each experiment were averaged to give the errors quoted above.

Supplementary Table S2. Affinity values for the binding of different variants of TPX2 to phosphorylated and dephosphorylated Aurora-A^{CA} as determined by ITC, showing the relative changes in affinity between Aurora-A phosphorylation state and between mutation of wild-type TPX2.

Aurora-A variant	N	TPX2 variant	K_d (μM)	X-fold change	X-fold change from WT value
Phosphorylated	0.95	WT	0.27 ± 0.04	9.1	n/a
Dephosphorylated	0.76	WT	2.46 ± 0.26		n/a
Phosphorylated	0.98	D11A	3.63 ± 0.18	9.8	13.4
Dephosphorylated	0.81	D11A	35.50 ± 6.34		14.4
Phosphorylated	0.45	F16A	4.57 ± 0.31	7.8	16.9
Dephosphorylated	0.10	F16A	35.69 ± 1.91		14.5
Phosphorylated	0.54	F35A	1.84 ± 0.07	1.8	6.8
Dephosphorylated	0.32	F35A	3.34 ± 0.25		1.4

N , the stoichiometry derived from the curve fitting of each interaction; K_d , dissociation constant. Aurora-A variant used is Aurora-A^{CA}. 'X-fold change' compares the affinity between the same TPX2 variants and phosphorylated or dephosphorylated Aurora-A^{CA}. 'X-fold change from WT value' compares the affinity between each TPX2 mutant and Aurora-A^{CA} to the wild-type TPX2-Aurora-A^{CA} affinity with Aurora-A^{CA} in the equivalent phosphorylation state. The errors given by Origin curve-fitting software for each experiment are either quoted above (for the mutant experiments, each performed once) or were averaged to give the errors quoted above (for the WT experiments, performed at least in triplicate).

Supplementary Table S3. Statistics from an X-ray crystallography based fragment screen against Aurora-A^{CA} at the XChem facility at Diamond Light Source.

	Fragments available	Crystals mounted	Datasets collected	Blobs detected	Hits identified	Hit rate
DSPL*	255	210	178	112	20	7.8 %
Maybridge†	1000	893	766	72	39	3.9 %
Total	1255	1103	944	184	59	4.7 %

* Diamond-SGC Poised Library. Soak concentration 200 mM.

† Maybridge commercial library. Soak concentration 80 mM.

Supplementary Table S4. NMR-STD analysis of the top 22 fragments from the X-ray crystallography based fragment screen

Frag No.	Peak ppm	Peak %	Peak S/N	Frag No.	Peak ppm	Peak %	Peak S/N
1		/		12		/	
2	7.52	0.94	4.54	13		/	
3	7.39	0.52	7.68	14	7.72	2.09	6.69
4	8.27	0.43	2.34	15		/	
5	7.70	3.61	37.97	16		/	
6	7.20	1.21	2.78	17	7.27	1.03	3.24
7	7.51	2.06	6.46	18	7.23	9.34	23.78
8	2.54	1.49	14.83	19		/	
9		/		20	7.73	2.90	6.10
10	7.45	4.15	18.65	21	1.27	1.43	7.64
11	7.71	6.95	14.95	22		/	

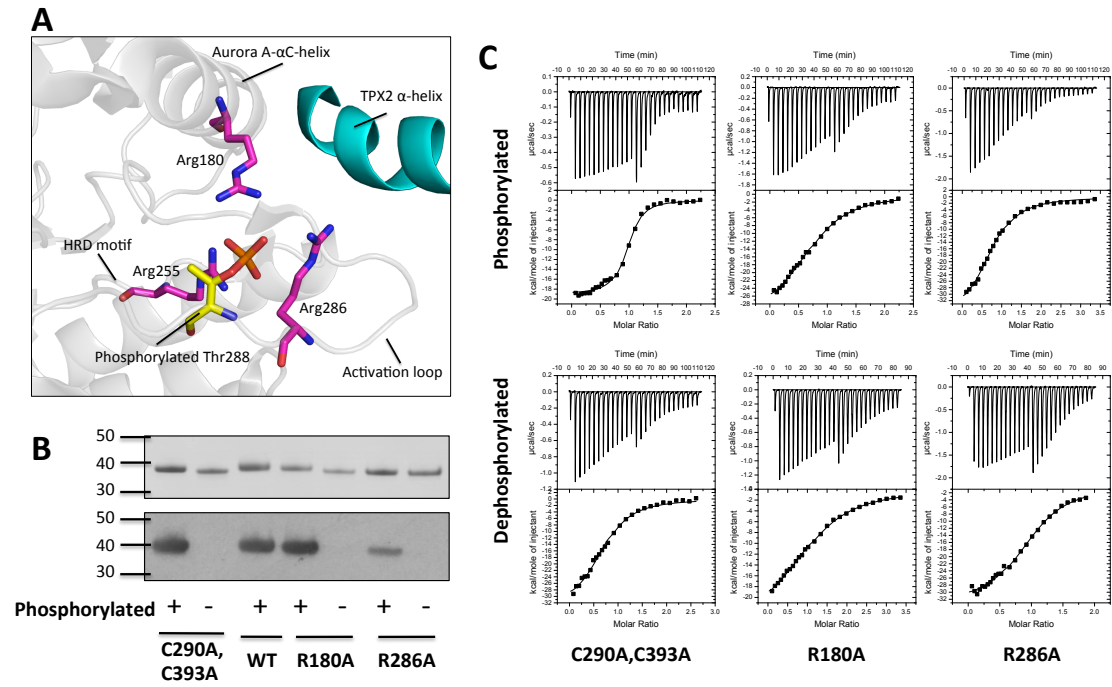
The peaks showing the highest signal/noise (S/N) ratio in a fragment's STD difference spectrum are described in this table. A slash indicates that no peaks could be seen in the STD difference spectrum with a S/N ratio over 2.00. Peak ppm, the chemical shift at which the chosen peak in the STD difference spectrum is seen; Peak %, the integral of the peak in the STD difference spectrum expressed as a percentage of the integral of the corresponding peak in the off-resonance spectrum, Peak S/N, the signal to noise ratio of the peak in the STD difference spectrum.

Supplementary Table S5. Binding data of five top-performing hits from an NMR-STD screen against Aurora-A^{CA}

Frag No.	Aurora-A Kd (μ M)	Aurora-A/CCT137690 Kd (μ M)	STD Intensity Aurora-A/CCT137690	STD Intensity Aurora-A/CCT137690/TPX2	STD Response Decrease
23	300	268	3.35 %	0.83 %	75.23 %
24	325	13399	2.16 %	0.64 %	70.18 %
25	444	1366	3.77 %	1.16 %	69.29 %
26	5132	1944	3.19 %	1.03 %	67.76 %
27	3081	2168	4.28 %	1.54 %	64.11 %

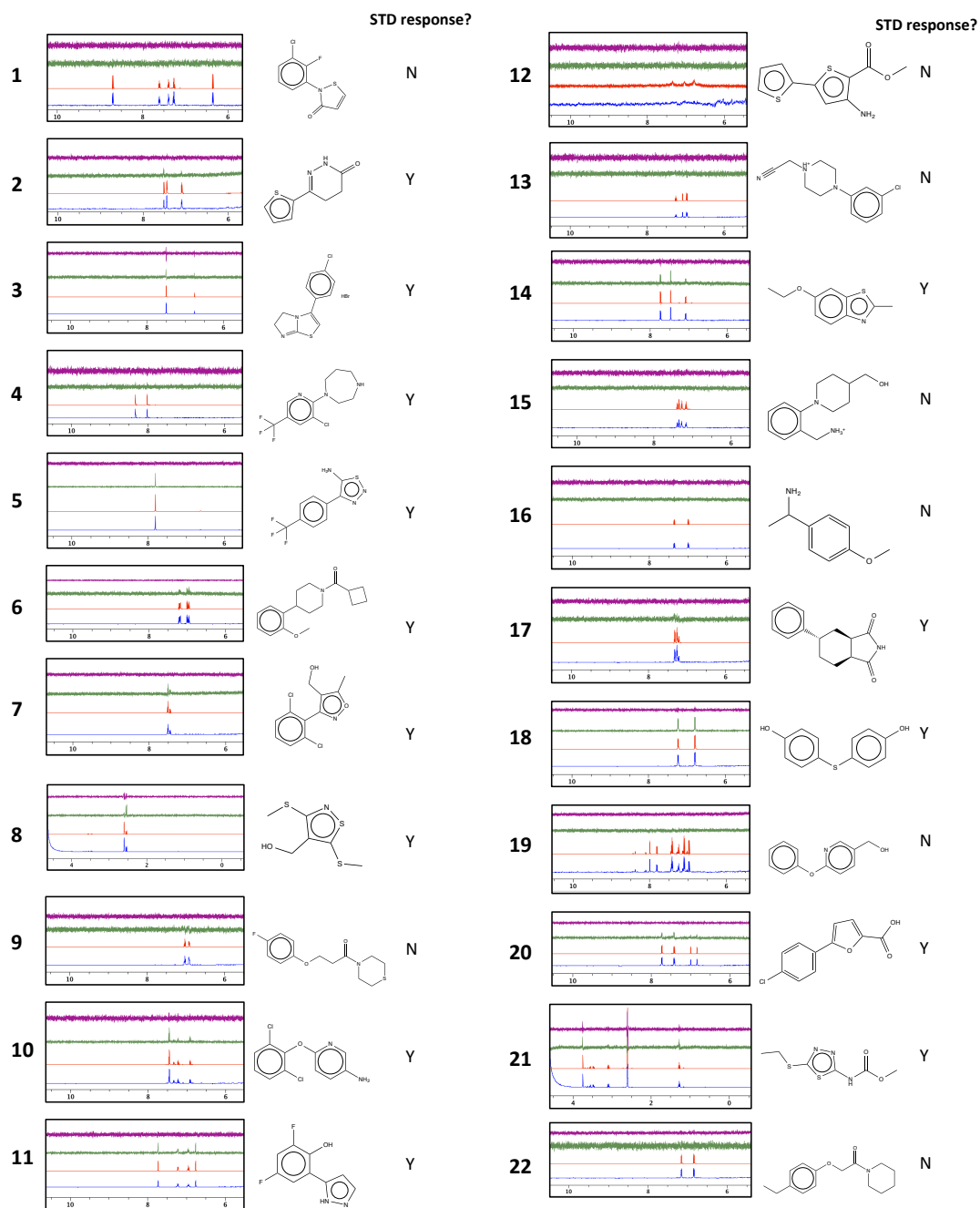
Kd, dissociation constant; all ITC experiments were performed in duplicate. STD experiments were conducted with Aurora-A at 5 μ M, fragment concentration at 500 μ M and final DMSO concentration at 2.5 % with fragments present in cocktails of 5 or 6 per sample. STD intensity was measured for each spectrum's largest peak against the corresponding peak in the non-saturated proton spectrum.

Supplementary Figure S1. Conformation of the Aurora-A (gray cartoon) activation loop when in complex with TPX2 (cyan cartoon), based on the crystal structure of the complex (PDB 1OL5). Interactions between the phosphate group of phosphorylated Thr288 (carbons colored yellow) and nearby arginine residues (carbons colored pink) help to stabilise the activation loop in a conformation compatible with the binding of TPX2. This may explain the 9-fold reduction in affinity between Aurora-A (gray) and TPX2 (cyan) upon dephosphorylation of Thr288. Salt bridges made between the phosphate group and the amine moieties of the arginine side-chains may act as a tether, holding the activation loop and α C-helix in a more rigid, organised conformation, necessary for efficient TPX2 binding (A). Role of Aurora-A phosphorylation in TPX2 binding: Different variants of Aurora-A were analysed by SDS-PAGE (top) and their phosphorylation state probed by Western blot using an antibody specific for phosphorylated Thr288 (Cell Signalling) (bottom) (B). Representative ITC traces showing the binding between phosphorylated or unphosphorylated (on Thr288) Aurora-A variants C290A/C393A, R180A and R286A and wild-type TPX2.

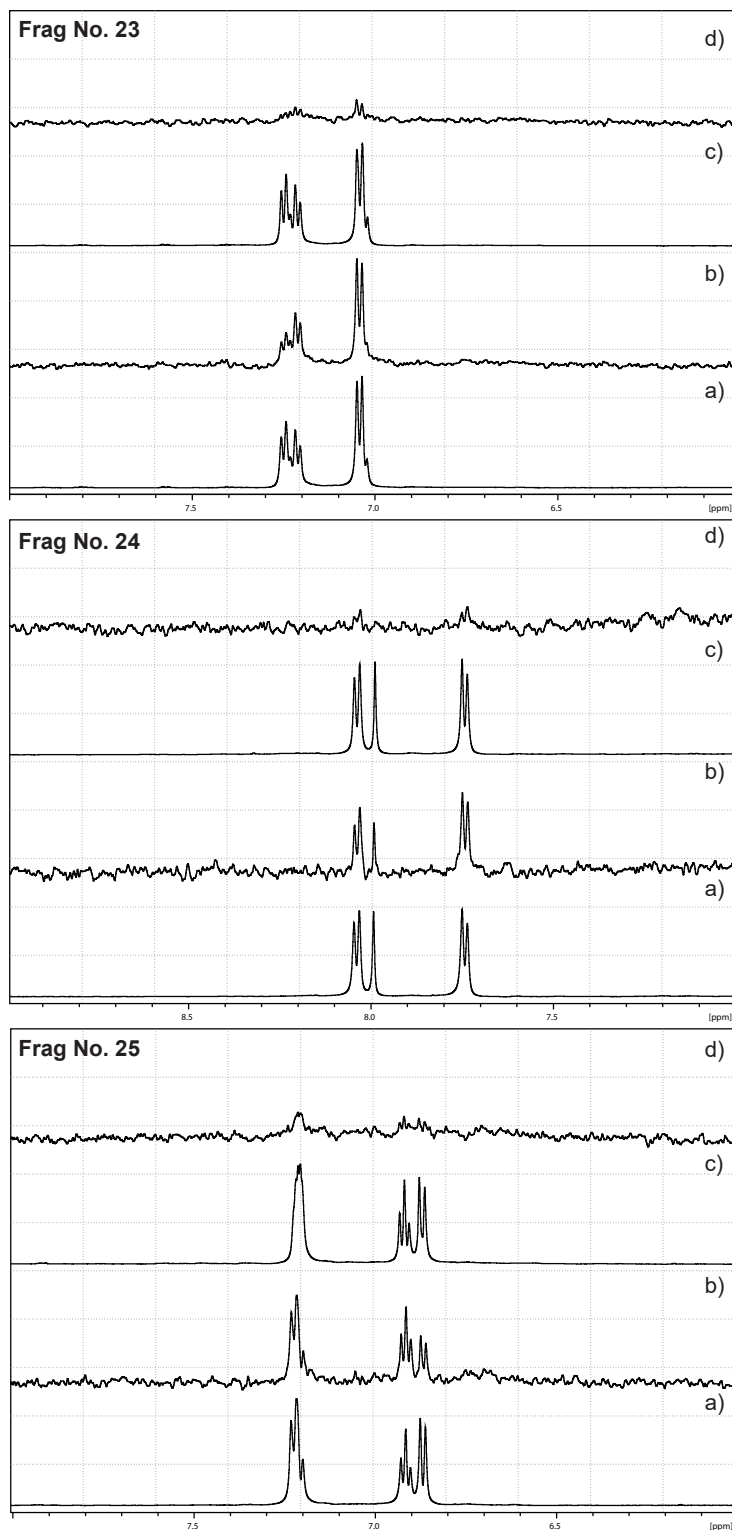


Supplementary Figure S2. STD responses of the 22 most promising hits against Aurora-A identified from X-ray crystallography based screen

Purple: STD difference spectrum of fragment no-protein control
 Green: STD difference spectrum of fragment + Aurora-A
 Red: Off-resonance STD spectrum of fragment + Aurora-A
 Blue: ¹H proton spectrum of fragment + Aurora-A



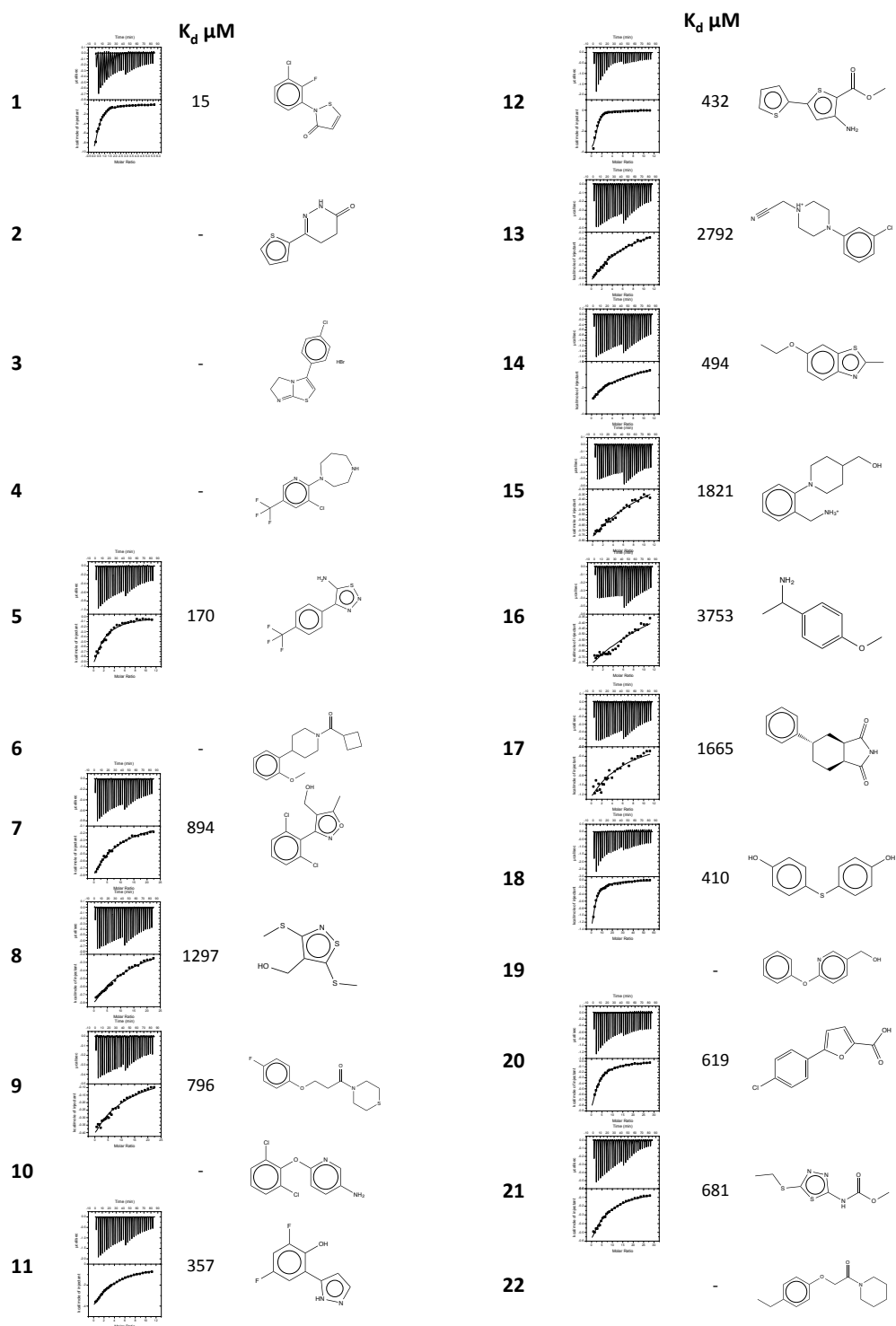
Supplementary Figure S3. STD responses of five top-performing hits from an STD-NMR screen against Aurora-A



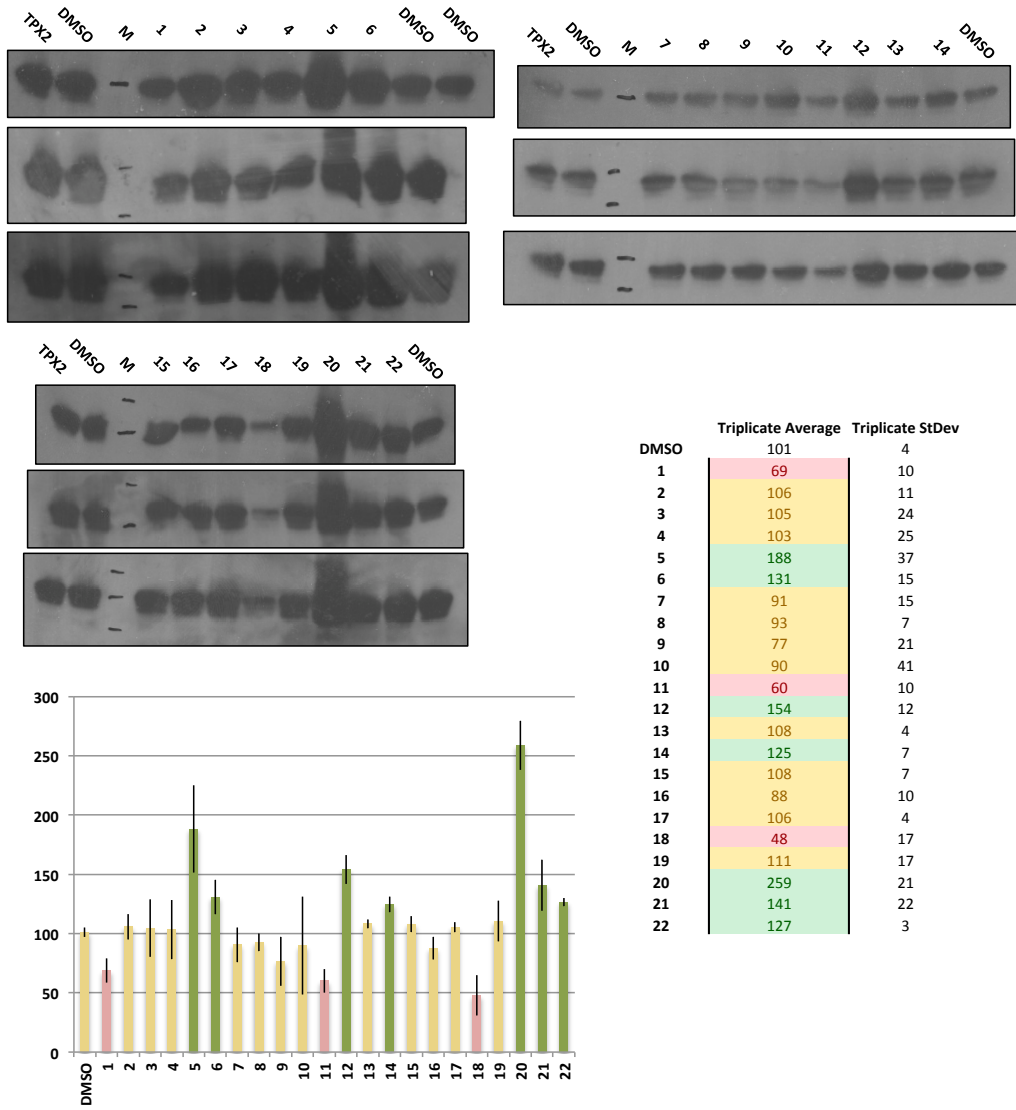
STD-NMR spectra in presence/absence of TPX2 binding partner for three most prominent fragment hits; a) ¹H reference spectrum in absence of TPX2, b) STD-NMR spectrum in absence of TPX2, c) ¹H reference spectrum in presence of TPX2; d) STD-NMR spectrum in presence of TPX2.

Decreased STD-NMR response in presence of TPX2 indicates the same binding site for both TPX2 and fragment hit.

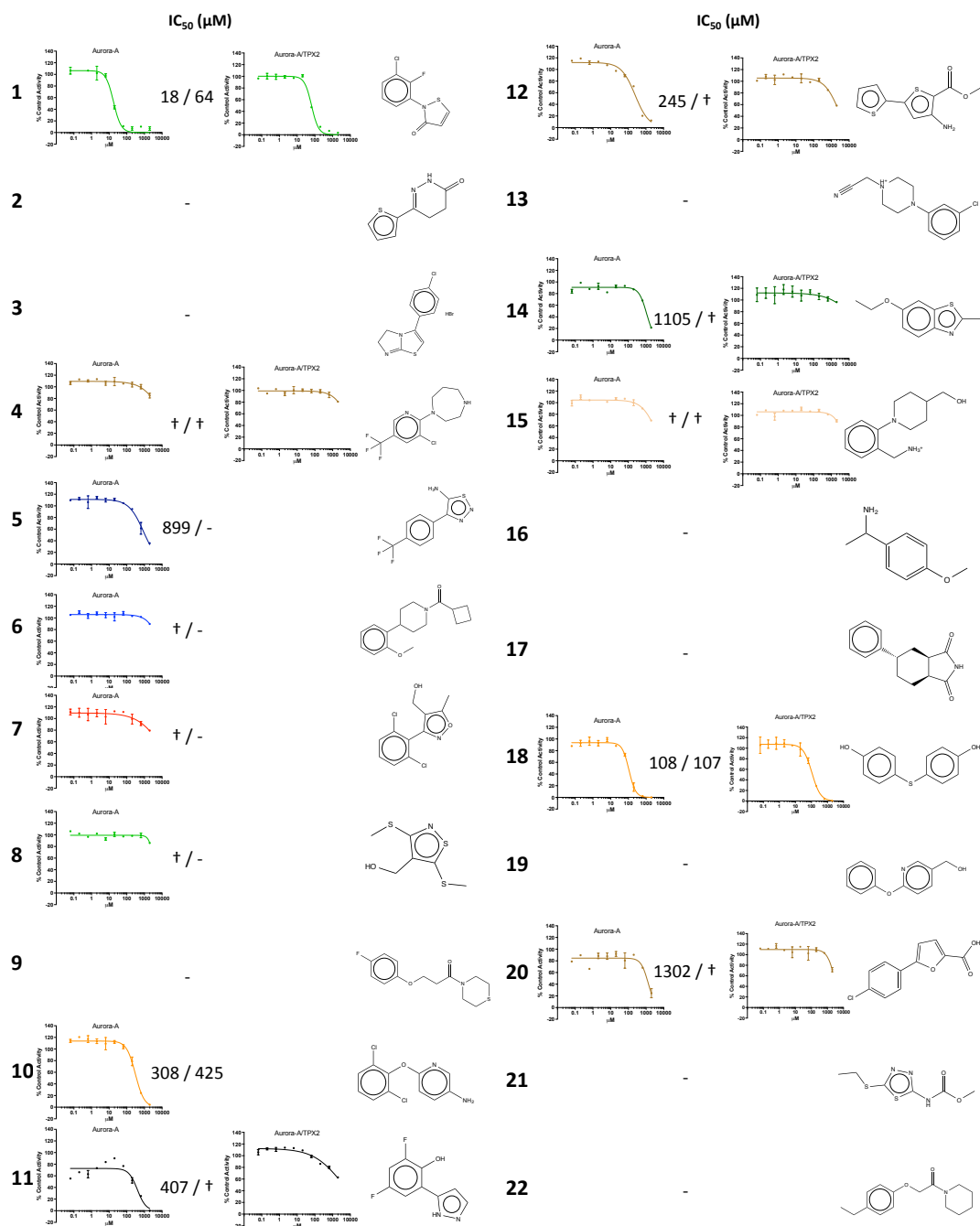
Supplementary Figure S4. Representative ITC isotherms reporting binding between fragments, as indicated, and Aurora-A. In each case fragment/buffer titration data has been subtracted from fragment/Aurora-A titration data. All curves were fitted with the stoichiometry between fragment and Aurora-A (N) fixed at 1.00 with the exception of fragment **1** ($N=0.43:1$).



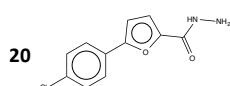
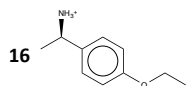
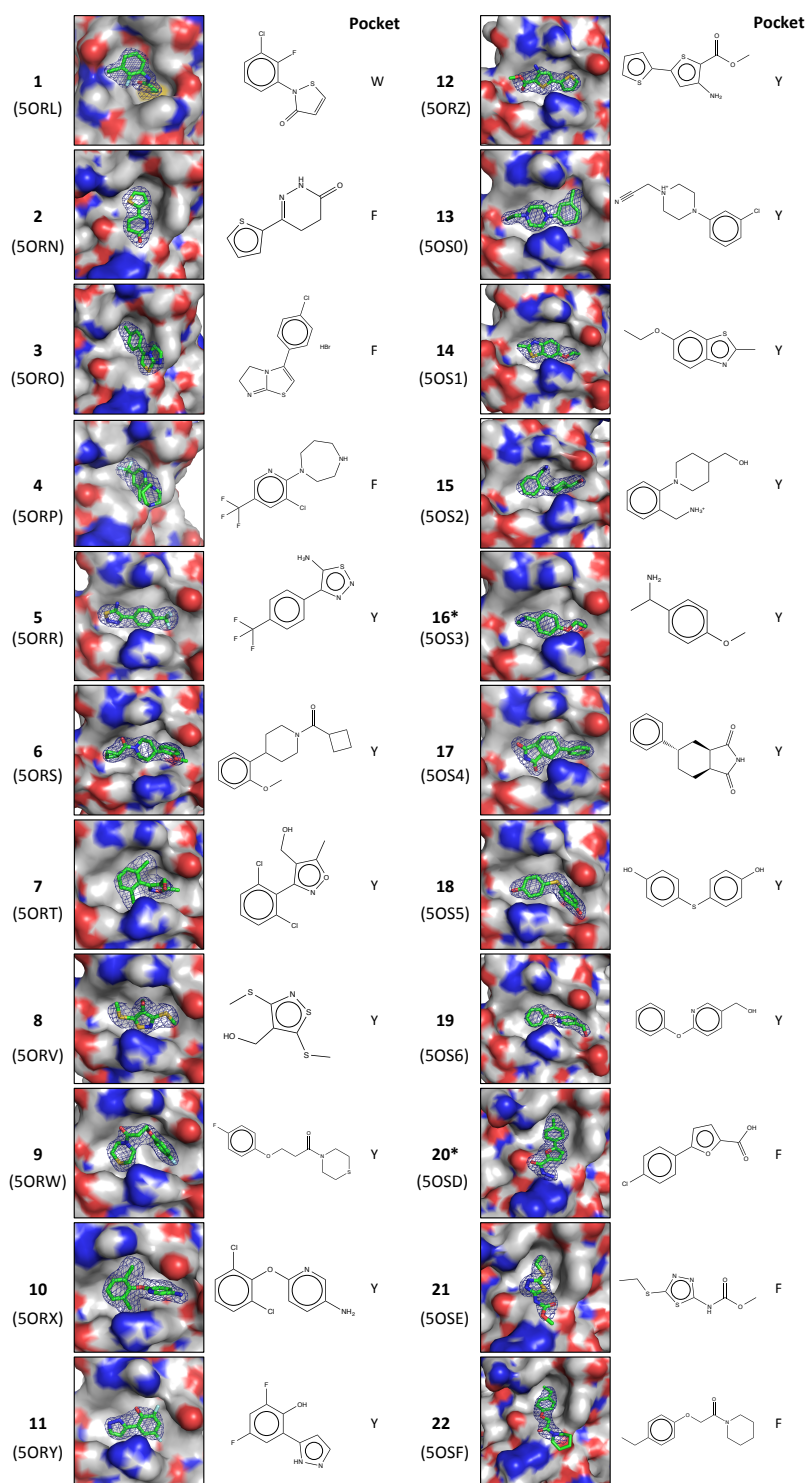
Supplementary Figure S5. Western blots of Aurora-A autophosphorylation in the presence of TPX2 and fragments. Each fragment (as indicated) was tested in triplicate and the average band densities expressed as a percentage of the average control (DMSO only) band density. Activators (green) were classified as over 125 % activation, inhibitors (red) as under 75 % activation and neither (yellow) as between these values



Supplementary Figure S6. ADP-Quest™ assays for inhibition of Aurora-A (left) and Aurora-A/TPX2 (right) activity by the top 22 fragments (as indicated). A dash indicates no inhibition of ATP turnover was seen and a cross indicates that the calculated IC₅₀ was above the maximum assay concentration of 2 mM.



Supplementary Figure S7. The chemical structures of the 22 Aurora-A-binding fragments are shown along with crystal structures indicating binding mode, electron density maps and PDB accession codes for the corresponding 22 Aurora-A/fragment complexes. The original fragment hits 16 and 20, for which analogues 16* and 20* were substituted, are shown underneath.



References

- (S1) Rowan, F. C., Richards, M., Bibby, R. A., Thompson, A., Bayliss, R., and Blagg, J. (2013) Insights into Aurora-A kinase activation using unnatural amino acids incorporated by chemical modification. *ACS Chem. Biol* **8**, 2184-2191.
- (S2) Burgess, S. G., and Bayliss, R. (2015) The structure of C290A:C393A Aurora A provides structural insights into kinase regulation. *Acta Crystallogr. F. Struct. Biol. Commun.* **71**, 315-319.
- (S3) Dodson, C. A., and Bayliss, R. (2012) Activation of Aurora-A kinase by protein partner binding and phosphorylation are independent and synergistic. *J. Biol. Chem.* **287**, 1150-1157.
- (S4) Bayliss, R., Sardon, T., Vernos, I., and Conti, E. (2003) Structural basis of Aurora-A activation by TPX2 at the mitotic spindle. *Mol. Cell.* **12**, 851-862.
- (S5) Ng, J.T., Dekker, C., Kroemer, M., Osborne, M. and von Delft, F. (2014) Using textons to rank crystallization droplets by the likely presence of crystals. *Acta Crystallogr. D Struct. Biol.* **70**, 2702-2718
- (S6) Collins, P. M., Ng, J. T., Talon, R., Nekrosiute, K., Krojer, T., Douangamath, A., Brandao-Neto, J., Wright, N., Pearce, N. M., and von Delft, F. (2017) Gentle, fast and effective crystal soaking by acoustic dispensing. *Acta Crystallogr. D Struct. Biol.* **73**, 246-255
- (S7) Pearce, N. M., Krojer, T., Bradley, A. R., Collins, P., Nowak, R. P., Talon, R., Marsden, B. D., Kelm, S., Shi, J., Deane, C. M., and von Delft, F. (2017) A multi-crystal method for extracting obscured crystallographic states from conventionally uninterpretable electron density. *Nat. Commun.* **8**, 15123
- (S8) Krojer, T., Talon, R., Pearce, N., Collins, P., Douangamath, A., Brandao-Neto, J., Dias, A., Marsden, B., and von Delft, F. (2017) The XChemExplorer graphical workflow tool for routine or large-scale protein-ligand structure determination. *Acta Crystallogr. D Struct. Biol.* **73**, 267-278
- (S9) Adams, P.D., Afonine, P.V., Bunkóczi, G., Chen, V.B., Davis, I.W., Echols, N., Headd, J.J., Hung, L.-W., Kapral, G.J., Grosse-Kunstleve, R.W., McCoy, A.J., Moriarty, N.W., Oeffner, R., Read, R.J., Richardson, D.C., Richardson, J.S., Terwilliger, T.C. and Zwart, P.H. (2010) PHENIX: a

comprehensive Python-based system for macromolecular structure solution.

Acta Crystallogr. D Biol. Crystallogr. **66**, 213-221

(S10) Emsley, P., Lohkamp, B., Scott, W.G. and Cowtan, K. (2010) Features and Development of Coot. *Acta Crystallogr. D Biol. Crystallogr* **66**, 486-501